

1 **Epigenetic drugs in somatostatin type 2 receptor radionuclide**
2 **theranostics and radiation transcriptomics in mouse**
3 **pheochromocytoma models**

4 – SUPPLEMENTAL INFORMATION –

5 Martin Ullrich¹, Susan Richter², Josephine Liers^{1,2}, Stephan Drukewitz^{3,4}, Markus
6 Friedemann², Jörg Kotzerke⁵, Christian G. Ziegler⁶, Svenja Nölting^{7,8}, Klaus Kopka^{1,9,10,11},
7 and Jens Pietzsch^{1,9}

8 ¹ Helmholtz-Zentrum Dresden-Rossendorf, Institute of Radiopharmaceutical Cancer Research, Department of
9 Radiopharmaceutical and Chemical Biology, Dresden, Germany

10 ² University Hospital Carl Gustav Carus at the Technische Universität Dresden, Institute of Clinical Chemistry
11 and Laboratory Medicine, Dresden, Germany

12 ³ National Center For Tumor Diseases/University Cancer Center Dresden, Core Unit for Molecular Tumor
13 Diagnostics, Dresden, Germany

14 ⁴ University of Leipzig Medical Center, Institute of Human Genetics, Leipzig, Germany

15 ⁵ University Hospital Carl Gustav Carus at the Technische Universität Dresden, Klinik und Poliklinik für
16 Nuklearmedizin, Dresden, Germany

17 ⁶ University Hospital Carl Gustav Carus at the Technische Universität Dresden, Department of Medicine III,
18 Dresden, Germany

19 ⁷ University Hospital Zurich (USZ) and University of Zurich (UZH), Department of Endocrinology, Diabetology
20 and Clinical Nutrition, Zurich, Switzerland

21 ⁸ University Hospital, LMU Munich, Department of Medicine IV, Munich, Germany

22 ⁹ Technische Universität Dresden, School of Science, Faculty of Chemistry and Food Chemistry, Dresden,
23 Germany

24 ¹⁰ German Cancer Consortium (DKTK), Partner Site Dresden, Dresden, Germany

25 ¹¹ National Center for Tumor Diseases (NCT), Partner Site Dresden, University Cancer Center (UCC), Dresden,
26 Germany

27 ***Abbreviated Title:*** Epigenetic SSTR2 modulation in PCC/PGL

28 ***Corresponding author and person to whom reprint requests should be addressed:***

29 Dr. Martin Ullrich

30 Helmholtz-Zentrum Dresden-Rossendorf

31 Institute of Radiopharmaceutical Cancer Research

32 Bautzner Landstraße 400, 01328 Dresden, Germany

33 Phone: +49-351-2604046, Fax: +49-351-26012622

34 E-mail: m.ullrich@hzdr.de

35 **Abbreviations:** A_v: volume activity resp. activity concentration; CT: X-ray computed
36 tomography; DAC: 5-Aza-2'-deoxycytidine; DNMT: DNA-N-methyltransferase; ET:
37 epigenetic treatment; GSEA: gene set enrichment analysis; HDAC: histone deacetylase; LD₅₀:
38 half-maximal lethal dose; MPC: mouse pheochromocytoma; MTT: mouse (MPC) tumor tissue-
39 derived; PCC/PGL: pheochromocytoma and paraganglioma; PET: positron emission
40 tomography; PRRT: peptide receptor radionuclide therapy; SPECT: single-photon emission
41 computed tomography; SSTR2: somatostatin type 2 receptor; SUV: standardized uptake value;
42 TATE: (Tyr³)octreotate; VPA: valproic acid

43 **Table of Content**

44 **1 Additional Methods..... 4**

45 1.1 Preparation of epigenetic drugs.....4

46 1.2 Radionuclide production and supply4

47 1.3 Tumor volumes in animal cohorts4

48 1.4 PET imaging and quantitative image analysis5

49 1.5 SPECT imaging and quantitative image analysis6

50 1.6 *Sstr2* promoter methylation analysis.....6

51 1.7 Pre-selection of KEGG pathways for gene set enrichment analysis.....7

52 1.8 Real-time RT-PCR.....7

53 **2 Additional Results 9**

54 2.1 [⁶⁸Ga]Ga-DOTA-TATE and [⁶⁴Cu]Cu-DOTA-TATE binding in response
55 to epigenetic drugs in vitro.....9

56 2.2 [⁶⁴Cu]Cu-DOTA-TATE uptake of allograft tumors in response to
57 epigenetic drugs10

58 2.3 [¹⁷⁷Lu]Lu-DOTA-TATE uptake and growth of allograft tumors in
59 response to epigenetic drugs17

60 2.4 Status of *Sstr2*/SSTR2 in allograft tumors in response to epigenetic drugs
61 and [¹⁷⁷Lu]Lu-DOTA-TATE20

62 2.5 Transcriptional responses of allograft tumors to epigenetic drugs and
63 [¹⁷⁷Lu]Lu-DOTA-TATE – all genes and gene sets included.....23

64 2.6 Transcriptional responses of allograft tumors to epigenetic drugs and
65 [¹⁷⁷Lu]Lu-DOTA-TATE – pre-selected gene sets involved in cancer and
66 radiation resistance.....26

67

68

69 **1 Additional Methods**

70 *1.1 Preparation of epigenetic drugs*

71 For *in vitro* application, VPA was freshly dissolved in cell culture medium and added to the
72 cells at final concentrations between 10^{-5} and 10^{-2} mol/L. DAC was dissolved in H₂O to obtain
73 a 10^{-4} mol/L stock solution that was stored at -20 °C. For each experiment, aliquots of the DAC
74 stock were thawed and added to the cells at final concentrations between 10^{-8} and 10^{-5} mol/L.

75 For *in vivo* application, VPA was dissolved at 0.26 mol/L in Dulbecco's phosphate-buffered
76 saline. DAC was dissolved at 0.04 mol/L in acetic acid (9.6 mol/L) to obtain a stock solution
77 that was further diluted to 6.6×10^{-4} mol/L in Dulbecco's phosphate buffered. All solutions
78 were adjusted to pH 7.2 using small amounts of aqueous NaOH (2.8 mol/L), sterile-filtered,
79 and frozen at -20 °C.

80 *1.2 Radionuclide production and supply*

81 The radionuclide ^{68}Ga ($[^{68}\text{Ga}]\text{GaCl}_3$ dissolved in 1 mol/L HCl) was obtained from the
82 commercial $^{68}\text{Ge}/^{68}\text{Ga}$ -Generator IGG 100-50M (Eckert und Ziegler). The radionuclide ^{64}Cu
83 ($[^{64}\text{Cu}]\text{CuCl}_2$ dissolved in 0.01 mol/L HCl) was produced at the Helmholtz-Zentrum Dresden-
84 Rossendorf on the cyclotron TR-Flex (Advanced Cyclotron Systems Inc., Richmond, Canada)
85 by a $^{64}\text{Ni}(p,n)^{64}\text{Cu}$ nuclear reaction. The radionuclide ^{177}Lu (EndolucinBeta[®], non-carrier
86 added $[^{177}\text{Lu}]\text{LuCl}_3$ dissolved in 0.04 mol/L HCl) was purchased from ITM (Isotope
87 Technologies München AG, München, Germany).

88 *1.3 Tumor volumes in animal cohorts*

89 Animals with higher initial tumor volume were specifically included in cohorts that received
90 epigenetic drugs in order to compensate for the growth-reducing effects of ET and to match
91 tumor volumes as closely as possible across cohorts at the time of radiopharmaceutical injection

92 (Table S 1). The variation in tumor volumes at a specific time point can be explained by
 93 different tumor formation times, while tumor growth rates were largely similar. Differences in
 94 tumor volume between the treatment groups were comparable to the overall variation observed
 95 in the entire model cohort.

96 **Table S 1: Tumor volumes of MPC and MTT allograft mice included in treatment groups;** (ET_{start}) day 0 of the treatment
 97 schedule when animals received the first dose of epigenetic drugs; (ET_{start} + 4 d \triangleq PET_{start} / PRRT_{start}) day 4 of the investigation
 98 when animals received a single dose of radiopharmaceutical to perform PET imaging or PRRT depending on the
 99 radiopharmaceutical applied; data presented as means \pm SEM

Cohort label	ET	Radiopharmaceutical	$V_{\text{tumor}} (\text{cm}^3)$	$V_{\text{tumor}} (\text{cm}^3)$
			ET _{start}	ET _{start} + 4 d \triangleq PET _{start} / PRRT _{start}
MPC allograft model – PET and biodistribution				
[Control]	Vehicle (PBS)	[⁶⁴ Cu]Cu-DOTA-TATE	0.18 \pm 0.12	0.28 \pm 0.13
[ET _{VPA}]	VPA	[⁶⁴ Cu]Cu-DOTA-TATE	0.27 \pm 0.13	0.46 \pm 0.23
[ET _{DAC}]	DAC	[⁶⁴ Cu]Cu-DOTA-TATE	0.39 \pm 0.16	0.57 \pm 0.18
[ET _{VPA+DAC}]	VPA + DAC	[⁶⁴ Cu]Cu-DOTA-TATE	0.51 \pm 0.17	0.81 \pm 0.20
MTT allograft model – PET and biodistribution				
[Control]	Vehicle (PBS)	[⁶⁴ Cu]Cu-DOTA-TATE	0.13 \pm 0.02	0.42 \pm 0.08
[ET _{VPA}]	VPA	[⁶⁴ Cu]Cu-DOTA-TATE	0.14 \pm 0.05	0.35 \pm 0.05
[ET _{DAC}]	DAC	[⁶⁴ Cu]Cu-DOTA-TATE	0.23 \pm 0.07	0.24 \pm 0.06
[ET _{VPA+DAC}]	VPA + DAC	[⁶⁴ Cu]Cu-DOTA-TATE	0.28 \pm 0.08	0.37 \pm 0.11
MPC allograft model – PRRT, SPECT, and gene expression				
[Control]	Vehicle (PBS)	w/o	0.17 \pm 0.03	0.39 \pm 0.03
[ET]	VPA + DAC	w/o	0.25 \pm 0.05	0.44 \pm 0.10
[PRRT]	Vehicle (PBS)	[¹⁷⁷ Lu]Lu-DOTA-TATE	0.09 \pm 0.01	0.24 \pm 0.06
[ET + PRRT]	VPA + DAC	[¹⁷⁷ Lu]Lu-DOTA-TATE	0.25 \pm 0.02	0.48 \pm 0.05
MTT allograft model – PRRT, SPECT, and gene expression				
[Control]	Vehicle (PBS)	w/o	0.13 \pm 0.02	0.54 \pm 0.05
[ET]	VPA + DAC	w/o	0.37 \pm 0.08	0.53 \pm 0.06
[PRRT]	Vehicle (PBS)	[¹⁷⁷ Lu]Lu-DOTA-TATE	0.12 \pm 0.01	0.36 \pm 0.04
[ET + PRRT]	VPA + DAC	[¹⁷⁷ Lu]Lu-DOTA-TATE	0.34 \pm 0.08	0.59 \pm 0.08

100 1.4 PET imaging and quantitative image analysis

101 Small animal positron emission tomography (PET) was performed using the nanoPET/CT
 102 scanner (Mediso Medical Imaging Systems, Budapest, Hungary). Images were reconstructed
 103 using the Tera-Tomo™ three-dimensional (3D) algorithm using a voxel size of 0.4 mm and
 104 applying corrections for scatter, attenuation, and decay. Images were post-processed and
 105 analyzed using ROVER (ABX, Radeberg, Germany). Three-dimensional volumes of interest

106 (VOIs) were created (40–60 min frames) applying fixed thresholds for delineation of tumor
107 (30%), muscle (0%), kidneys (25%), and liver (35%).

108 *1.5 SPECT imaging and quantitative image analysis*

109 Small animal single-photon emission computed tomography nanoSPECT/CT was performed
110 using the nanoSPECT/CT scanner (Mediso Medical Imaging Systems) equipped with the
111 APT62 aperture consisting of four M3 multi-pinhole collimators providing a 30×30 mm axial
112 field of view (FOV). Photon emission was recorded using a frame time of 120 s (total scan time
113 of 90 min) and binned within the 20% energy windows of the 56, 113, and 208 keV photopeaks.
114 Images were reconstructed using the Tera-Tomo™ three-dimensional (3D) algorithm at high
115 dynamic range using a voxel size of 0.4 mm and applying corrections for scatter and
116 attenuation. Images were post-processed and analyzed using ROVER (ABX). Three-
117 dimensional VOIs were created by applying a fixed threshold for delineation of tumor (20%),
118 kidneys (15%), and liver (25%).

119 *1.6 Sstr2 promoter methylation analysis*

120 DNA from cell cultures and allografts was extracted using the DNeasy Blood and Tissue Kit
121 (Qiagen, Venlo, The Netherlands) and treated with bisulfite using the EpiTect Fast DNA
122 Bisulfite Kit (Qiagen, Hilden, Germany). Bisulfite-converted DNA was amplified using a
123 primer pair covering 20 CpGs of the *Sstr2* promoter. Amplicon size (195bp) was confirmed
124 on an agarose gel and the PCR product was sent for Sanger sequencing (Microsynth, Balbach,
125 Switzerland). Electropherograms were compared to PCR products amplified from bisulfite-
126 converted mouse Universal Methylated DNA Standard (Zymoresearch, Irvine CA, USA) and
127 an unmethylated 900bp-DNA fragment. The latter was generated by amplification of genomic
128 mouse DNA using primers annealing around the CpG island of *Sstr2*. Nucleotide sequences
129 of primers are provided in (Table S 2).

130 **Table S 2: Primer pairs used for *Sstr2* promoter methylation analysis**

Target	Nucleotide sequence
Amplification of bisulfite-converted DNA	5'-AtTtTGtTtAtCGGGTttAAAtAGGAtt-3' 5'-CCTaTAaATCATTaACGCCCAaCC-3'
Generation of an unmethylated DNA fragment	5'-GGTTGGGCTGGGGCTGGGTC-3' 5'- CCTCGAGCACTCGCTTCCCTGTG-3'

131 *1.7 Pre-selection of KEGG pathways for gene set enrichment analysis*

132 For investigations on transcriptional responses associated with ET and PRRT, 39 pathways
 133 were pre-selected from the KEGG database for gene set enrichment analysis. The latter included
 134 the following two categories: (1) pathways involved in cancer ('pathways in cancer'
 135 [mmu05200 and pathways therein]; 'transcriptional misregulation in cancer' [mmu05202]) and
 136 (2) pathways involved in the sensitivity to ionizing radiation (central carbon metabolism in
 137 cancer [mmu5230 and pathways therein]; DNA damage repair [mmu03030, mmu03410,
 138 mmu03420, mmu03430, mmu03440, mmu03450, mmu03460]; reactive oxygen species (ROS)
 139 defense [mmu00480]).

140 A specific subset of these enrichment pathways was extracted representing the additional effects
 141 of ET on the regular response to PRRT. These gene sets met two conditions: (i) enrichment in
 142 [ET + PRRT] vs. [PRRT], *and* at the same time (ii) overlapping with enrichment in [PRRT] vs.
 143 [Control] *or* with enrichment in [ET + PRRT] vs. [Control]. Differentially expressed leading-
 144 edge genes from the extracted enrichment pathways were reported.

145 *1.8 Real-time RT-PCR*

146 cDNA was prepared from mouse RNA using qScript cDNA Synthesis Kit (Quantabio, Beverly
 147 MA, USA) following the manufacturer's recommendations. cDNA was diluted 1:2 and
 148 amplified with the PerfeCTa SYBR Green Super Mix Low Rox (Quantabio, Beverly MA, USA)
 149 on a CFX Connect Real-Time PCR Detection System (Bio-Rad, Hercules CA, USA) using
 150 primer pairs specific for *Sstr2*, *Chga*, *Actb*, and *Rpl19* (Table S 3). Amplicons were generated

151 in 40 cycles (95°C 5 sec, 60°C 10 sec) with 5 minutes at 95°C for initial denaturation and
152 characterized by melting curve analysis and on an agarose gel.

153 **Table S 3: Primer pairs used for real-time RT-PCR**

Target gene	Nucleotide sequence
<i>Sstr2</i>	5'-CGCATGGTGTCCATCGTAGT-3' 5'-GGATTGTGAATTGTCTGCCTTGA-3'
<i>Chga</i>	5'-CCAAGGTGATGAAGTGCCTC-3' 5'-GGTGTCCGAGGATAGAGAGGA-3'
<i>Actb</i>	5'-GGCTGTATTCCCCTCCATCG-3' 5'-CCAGTTGGTAACAATGCCATGT-3'
<i>Rpl19</i>	5'-ATATGGGCATAGGGAAGAGG-3' 5'-CTGTCTGCCTTCAGCTTGT-3'

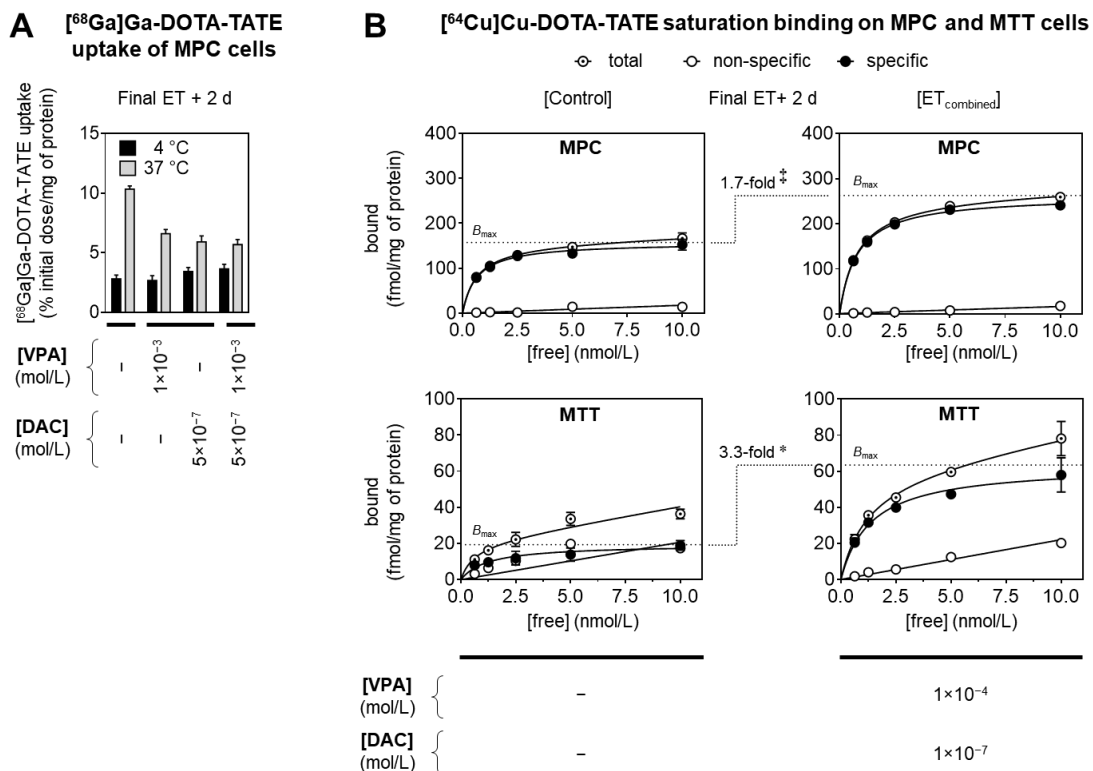
154

155 **2 Additional Results**

156 **2.1 $[^{68}\text{Ga}]\text{Ga-DOTA-TATE}$ and $[^{64}\text{Cu}]\text{Cu-DOTA-TATE}$ binding in response to epigenetic**
 157 **drugs in vitro**

158 In MPC cells, the radioligand assay showed impairment of $[^{68}\text{Ga}]\text{Ga-DOTA-TATE}$ uptake at
 159 37°C due to cytotoxic effects of VPA and DAC at concentrations of 10^{-3} mol/L and
 160 $5\times 10^{-7}\text{ mol/L}$, respectively. Hence the following experiments were performed with lower
 161 concentrations of the epigenetic drugs (Figure S 1A).

162 Binding assays with cell homogenates showed that ET, a combination of 10^{-4} mol/L VPA and
 163 10^{-7} mol/L DAC, significantly increased the specific binding capacity for $[^{64}\text{Cu}]\text{Cu-DOTA-}$
 164 TATE in both MPC and MTT cells (Figure S 1B).



165 **Figure S 1: SSTR2 radiotracer assays and effects of epigenetic drugs; (A)** Decreased $[^{68}\text{Ga}]\text{Ga-DOTA-TATE}$ uptake in
 166 MPC cells at 37°C after treatment with VPA and DAC at concentrations of 10^{-3} mol/L and $5\times 10^{-7}\text{ mol/L}$, respectively;
 167 **(B)** Saturation binding of $[^{64}\text{Cu}]\text{Cu-DOTA-TATE}$ in homogenates of MPC and MTT cells treated with VPA and DAC at
 168 concentrations of 10^{-4} mol/L and 10^{-7} mol/L , respectively; (dotted lines) B_{max} values of SSTR2 binding sites; significance of
 169 differences (t-test): * $P < 0.05$; ‡ $P < 0.01$
 170

171 2.2 [⁶⁴Cu]Cu-DOTA-TATE uptake of allograft tumors in response to epigenetic drugs

172 PET images of MPC and MTT allograft mice provide an overview over ET effects on the
173 distribution of [⁶⁴Cu]Cu-DOTA-TATE in individual animals (Figure S 2). Quantitative image
174 analysis showed the reduction of [⁶⁴Cu]Cu-DOTA-TATE uptake in MPC tumors and the
175 stimulation of [⁶⁴Cu]Cu-DOTA-TATE in MTT tumors in response to ET. Extracted
176 standardized uptake values (SUV_{mean}, SUV_{max}) showed similar trends to reference tissue
177 ratios (tumor/muscle). (Table S 4). Uptake values in tumors measured *ex vivo* (SUV and
178 % initial dose/g tissue) confirmed these observations (Figure S 3).

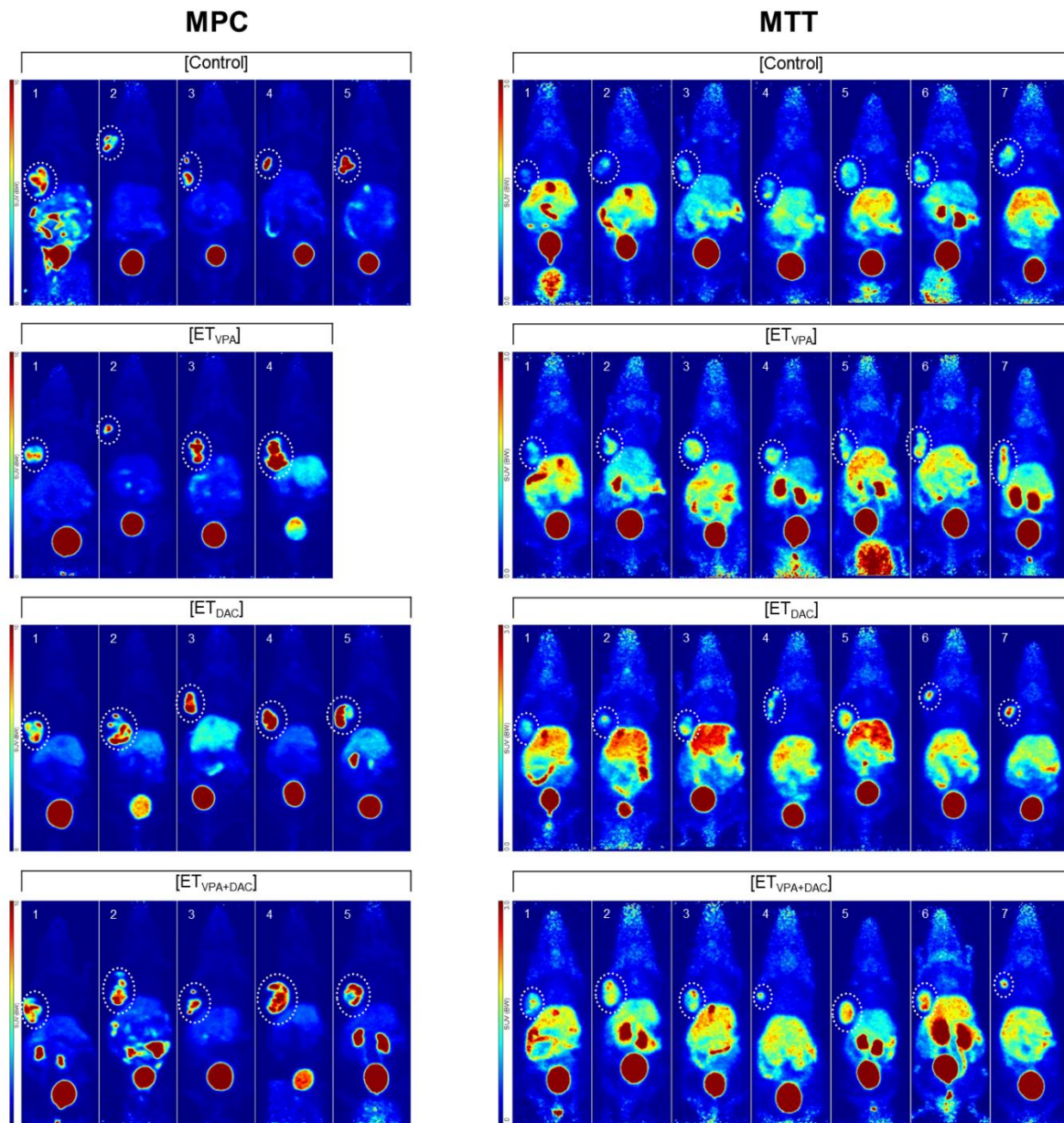
179 Uptake of [⁶⁴Cu]Cu-DOTA-TATE in tumors was correlated with other parameters such as
180 initial tumor, ET-induced reduction in tumor growth, and ET-induced changes in the
181 biodistribution of the radiotracer. Tumor growth was reduced upon ET in both MPC and MTT
182 allograft mice (Figure S 4A). Since correlation analyses did not show any relationship
183 between tumor volume and the SUV (Figure S 4B), animals with tumor volumes of
184 0.05–1.4 cm³ for MPC and 0.04–0.82 cm³ for MTT were included in quantitative image
185 analyses focusing on [⁶⁴Cu]Cu-DOTA-TATE uptake. A positive linear relationship between
186 growth-reducing effects of ET and reduced SUVs in MPC tumors indicate that cytostatic
187 effects of the epigenetic drugs contributed to the reduction of [⁶⁴Cu]Cu-DOTA-TATE uptake
188 (Figure S 4C).

189 Using the treatment protocol, epigenetic drugs showed no statistically relevant effects on
190 [⁶⁴Cu]Cu-DOTA-TATE retention in blood as determined from areas under time-activity
191 curves (AUC_{0–60 min}) in the heart, nor did individual differences in activity retention in blood
192 correlate with SUV changes in tumors (Figure S 5A–B).

193 Activity retention in the liver was significantly higher in DAC-treated animals; however, this
194 effect showed no relationship with SUV changes in tumors (Figure S 5C–D). Activity in the

195 liver may also have resulted from [⁶⁴Cu]Cu²⁺ trans-chelation reactions and small amounts of
196 free [⁶⁴Cu]Cu²⁺ ions (< 3%) remaining in the radiotracer preparation.

197 Activity in the renal cortex showed no statistically relevant differences between treatment
198 groups nor did individual differences correlate with SUV changes in tumors (Figure S 5E–F).
199 Some animals showed higher activity in the renal pelvis, resulting from activity in primary
200 urine that has not yet been drained completely.



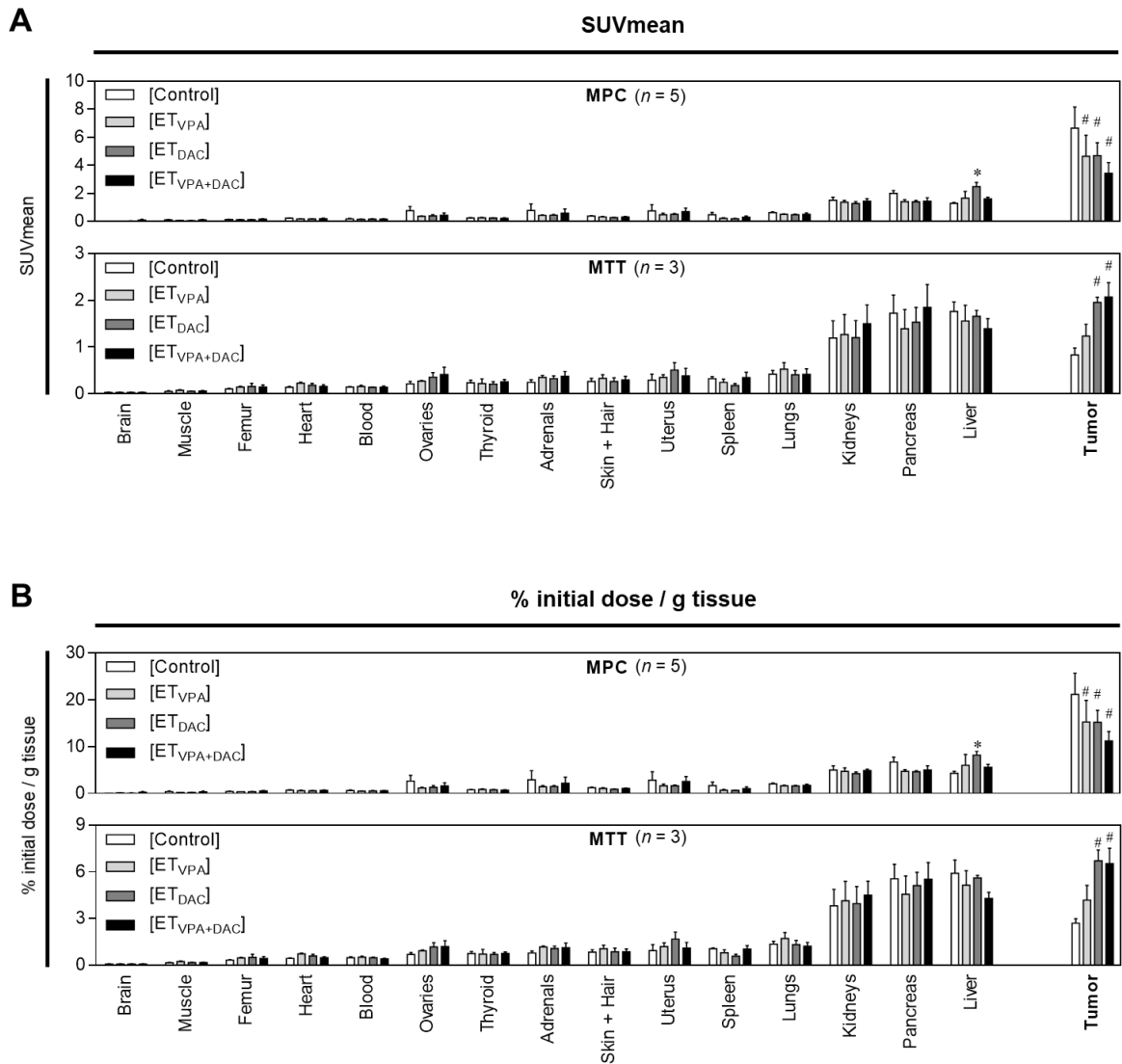
201
 202 **Figure S 2: PET images of $[^{64}\text{Cu}]\text{Cu-DOTA-TATE}$ distribution in MPC and MTT allograft mice in response to**
 203 **epigenetic treatment;** Maximum intensity projections presented with different SUV color scaling: MPC (0–10); MTT (0–3);
 204 ET: treatment with VPA (250 mg/kg) and DAC (1 mg/kg) as single and combination doses, respectively, on days –3 and 0;
 205 PET imaging with $[^{64}\text{Cu}]\text{Cu-DOTA-TATE}$ (10 MBq/animal, equivalent to 0.25 nmol) on day 1 after final ET; MPC allograft
 206 mice [Control #1 and #5] and [ET VPA+DAC #2] showed activity hotspots within the intestinal loops resulting from accidental
 207 intake of contaminated bedding materials assimilated prior to PET scanning (between radiotracer injection and induction of
 208 anesthesia); (dotted regions) radiotracer uptake in tumors 40–60 min after injection; see Table S 4 for uptake values in tumors

209 **Table S 4: Uptake of [⁶⁴Cu]Cu-DOTA-TATE in tumors of MPC and MTT allograft mice treated with epigenetic drugs;**
 210 ET: treatment with VPA (250 mg/kg) and DAC (1 mg/kg) as single and combination doses, on days -3 and 0; PET imaging
 211 with [⁶⁴Cu]Cu-DOTA-TATE (10 MBq/animal, equivalent to 0.25 nmol) on day 1 after final ET; (SUV) standardized uptake
 212 values 40–60 min after injection of the radiotracer

Cohort label	Animals	SUVmean tumor	SUVmean ratio tumor / muscle	SUVmax tumor	SUVmax ratio tumor / muscle
MPC allograft mice					
[Control]	1	5.71	61.5	12.5	62.4
	2	6.16	56.4	13.8	51.5
	3	8.04	85.8	19.2	83.4
	4	9.46	112	18.8	63.8
	5	10.3	103	22.7	106
	mean ± SEM	7.93 ± 0.89	83.8 ± 11.0	17.4 ± 1.89	73.3 ± 9.54
[ET _{VPA}]	1	4.22	60.0	8.80	33.0
	2	5.61	67.2	10.8	60.8
	3	8.55	91.2	19.7	78.3
	4	9.24	100	18.5	65.2
	mean ± SEM	6.91 ± 1.19	79.6 ± 9.53	14.5 ± 2.73	59.3 ± 9.54
[ET _{DAC}]	1	5.09	68.2	11.5	57.8
	2	6.74	96.7	13.9	65.6
	3	7.52	93.2	15.3	58.7
	4	7.99	80.6	15.2	69.1
	5	9.57	104	20.6	67.9
	mean ± SEM	7.38 ± 0.74	88.6 ± 6.39	15.3 ± 1.49	63.8 ± 2.35
[ET _{VPA+DAC}]	1	5.89	73.7	13.2	47.4
	2	6.11	82.3	13.2	66.9
	3	6.63	70.9	13.4	57.6
	4	7.04	79.7	15.2	63.3
	5	7.48	90.0	16.0	72.2
	mean ± SEM	6.63 ± 0.29	79.3 ± 3.36	14.2 ± 0.58	61.5 ± 4.24
MTT allograft mice					
[Control]	1	0.12	1.32	0.25	1.09
	2	0.43	4.91	1.02	4.05
	3	0.54	8.63	1.33	4.52
	4	0.55	6.83	1.39	6.57
	5	0.60	7.64	1.53	9.62
	6	0.68	9.13	1.67	6.34
	7	0.68	8.43	1.63	8.38
	mean ± SEM	0.51 ± 0.07	6.70 ± 1.04	1.26 ± 0.19	5.80 ± 1.08
[ET _{VPA}]	1	0.34	3.20	0.69	3.3
	2	0.70	10.52	1.41	4.72
	3	0.71	7.63	1.61	8.25
	4	0.73	11.4	1.60	10.8
	5	0.74	7.80	1.62	5.31
	6 ^R	0.86	9.73	1.73	5.70
	7 ^R	1.06	9.95	2.23	6.06
	mean ± SEM	0.73 ± 0.08	8.60 ± 1.04	1.55 ± 0.17	6.30 ± 0.94
[ET _{DAC}]	1	0.38	4.91	0.83	4.01
	2	0.65	7.82	1.52	6.62
	3	0.77	8.27	1.66	5.31
	4 ^R	0.80	12.6	2.00	11.0
	5 ^R	0.93	11.5	1.88	7.68
	6 ^R	1.24	17.9	2.71	14.7
	7 ^R	1.37	21.3	2.72	18.9
	mean ± SEM	0.88 ± 0.13 *	12.1 ± 2.2 *	1.90 ± 0.25	9.74 ± 2.05
[ET _{VPA+DAC}]	1	0.74	8.72	1.68	7.80
	2 ^R	0.97	10.8	2.31	8.84
	3 ^R	0.99	9.47	2.44	10.7
	4 ^R	1.02	10.8	2.34	8.98
	5 ^R	1.19	13.1	2.34	11.8
	6 ^R	1.24	10.7	2.81	7.75
	7 ^R	1.27	16.6	2.88	15.0
	mean ± SEM	1.06 ± 0.07 #	11.5 ± 1	2.40 ± 0.15 ‡	10.1 ± 0.99

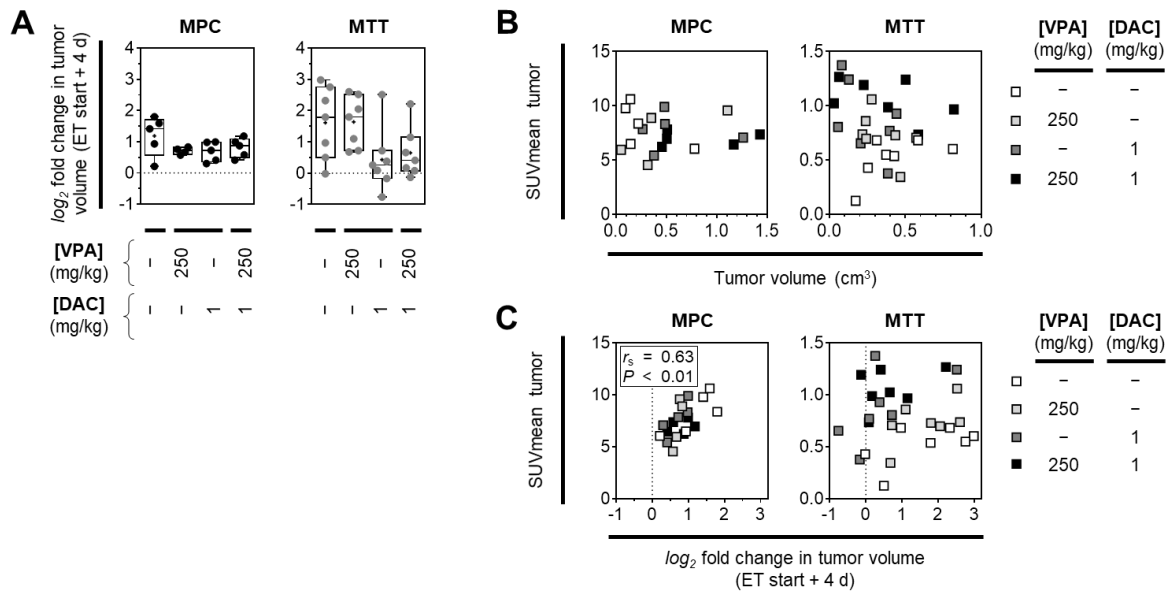
213 ^R SUV responders to epigenetic treatment; responder thresholds were calculated from the SUVmean values of the [Control]
 214 cohorts + two times typical error (2×TE)

215 * Significance of differences compared to [Control]: **P* < 0.05; ‡ *P* < 0.01; # *P* < 0.001



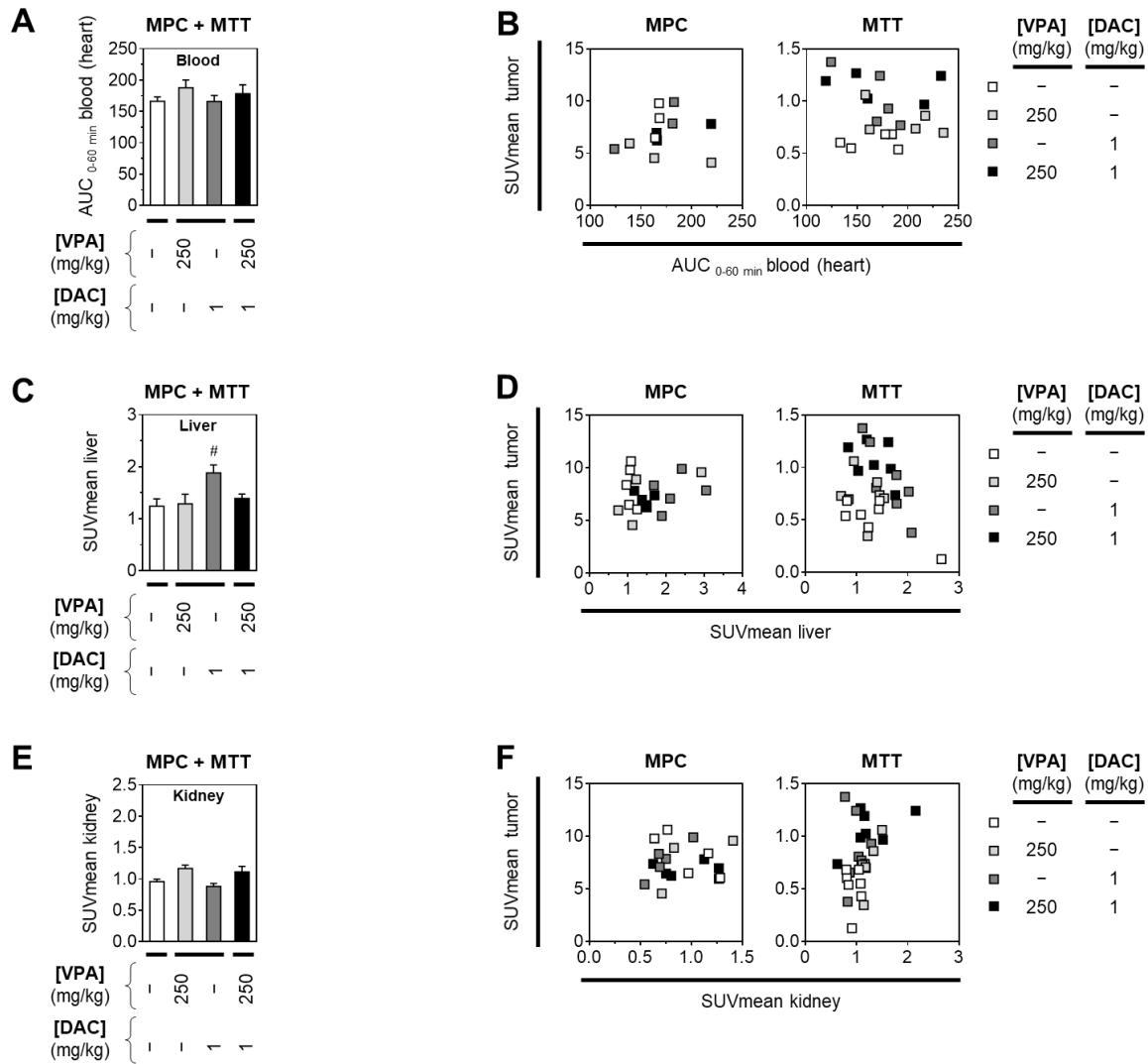
216
217
218
219
220
221

Figure S 3: Distribution of $[^{64}\text{Cu}]\text{Cu-DOTA-TATE}$ in MPC and MTT allograft mice treated with epigenetic drugs as measured *ex vivo* in tissue samples; (A) Radiotracer distribution reported as standardized uptake values; (B) Radiotracer distribution reported as % initial dose/g tissue; both evaluation methods showed similar effects of ET with increased tumor uptake in MTT allograft mice only; significance of differences: # $P < 0.001$



222
223
224
225
226
227
228
229

Figure S 4: Correlation analyses between uptake of $[^{64}\text{Cu}]\text{Cu-DOTA-TATE}$ in tumors and tumor growth in MPC and MTT allograft mice treated with epigenetic drugs; (A) Changes in tumor volume in response to ET showing reduced growth in both MPC and MTT allograft mice; (\log_2 fold changes) number of volume doublings compared to ET start; (B) Correlation analyses showing independence of radiotracer uptake in tumors (SUVmean) from tumor volumes (cm^3) across all treatment groups; (C) Correlation analyses showing a positive linear relationship between the growth-reducing effects of ET and reduced radiotracer uptake (SUVmean) in MPC tumors



230

231

232

233

234

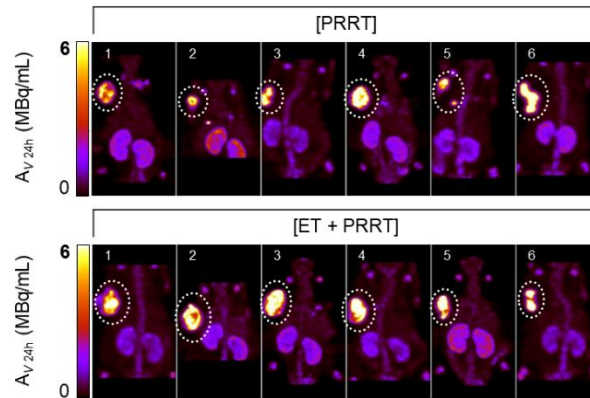
235

Figure S 5: Correlation analyses between uptake of $[^{64}\text{Cu}]\text{Cu-DOTA-TATE}$ in tumors and retention in blood, liver, and kidneys in MPC and MTT allograft mice treated with epigenetic drugs; (A–B) Activity retention in blood determined from areas under time-activity curves ($\text{AUC}_{0-60 \text{ min}}$) in the heart and correlation with tumor uptake; (C–D) Activity retention in the liver and correlation with tumor uptake; (E–F) Activity retention in the renal cortex and correlation with tumor uptake; significance of differences: # $P < 0.001$

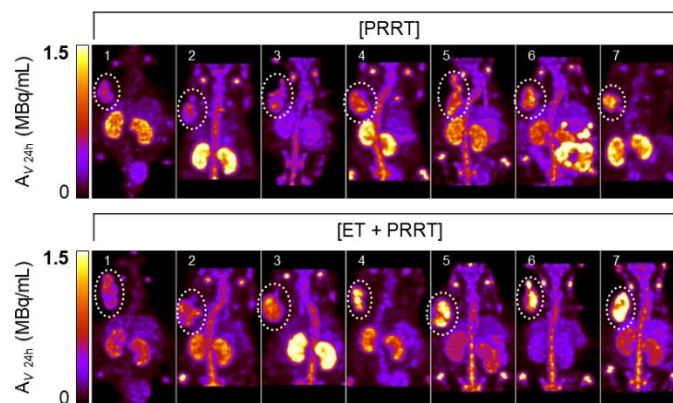
236 2.3 [¹⁷⁷Lu]Lu-DOTA-TATE uptake and growth of allograft tumors in response to epigenetic
237 drugs

238 SPECT images of MPC and MTT allograft mice provide an overview over ET effects on the
239 distribution of [¹⁷⁷Lu]Lu-DOTA-TATE in individual animals (Figure S 6). Excretion of the
240 radiotracer via the renal pathway was associated with some retention of activity in the renal
241 cortex. Small amounts of free [¹⁷⁷Lu]Lu³⁺ ions (< 5%) that remained in the radiotracer
242 preparation contributed to retention of activity in liver and bones, in particular in joints.
243 Quantitative image analysis showed no effect of ET on [¹⁷⁷Lu]Lu-DOTA-TATE uptake in
244 MPC tumors but a higher uptake in MTT tumors. Analyses of VOI-averaged activity
245 concentrations (A_V mean) and activity hotspots (A_V max) in tumors showed similar trends
246 (Table S 5).

MPC



MTT



247

248

249

250

251

252

253

254

255

Figure S 6: SPECT images of $[^{177}\text{Lu}]\text{Lu-DOTA-TATE}$ distribution in MPC and MTT allograft mice and effects of epigenetic treatment; Maximum intensity projections presented at different A_V color scaling: MPC (0–6 MBq/mL); MTT (0–1.5 MBq/mL); ET: treatment with VPA (250 mg/kg) and DAC (1 mg/kg) as combination doses on days –4 and –1; PRRT: treatment with $[^{177}\text{Lu}]\text{Lu-DOTA-TATE}$ (70 MBq/animal, equivalent to 1.2 nmol) as a single dose on day 0; quantitative SPECT imaging on day 1; (A_V 24 h) activity concentration of radionuclide drug 24 hours after injection; (dotted regions); MTT allograft mouse [PRRT #6] showed activity hotspots within the stomach and the intestinal loops resulting from accidental intake of contaminated bedding materials assimilated prior to image recording (between injection of radiopharmaceutical and initiation of anesthesia); see Table S 5 for tumor uptake values and follow-up of tumor growth in individual animals

256 **Table S 5: Uptake of [¹⁷⁷Lu]Lu-DOTA-TATE in tumors and follow-up of tumor growth in MPC and MTT allograft**
 257 **mice treated with epigenetic drugs; ET: treatment with VPA (250 mg/kg) and DAC (1 mg/kg) as combination doses on**
 258 **days -4 and -1; PRRT: treatment with [¹⁷⁷Lu]Lu-DOTA-TATE (70 MBq/animal, equivalent to 1.2 nmol) as a single dose on**
 259 **day 0; (A_{V 24h}) activity concentration of the radionuclide drug 24 hours after injection; mRNA of tumors was obtained from**
 260 **the sub-cohorts A-H**

Cohort label	Animals entire cohort	Animals sub-cohort (mRNA samples) ¹	A _V mean _{24h} tumor (MBq/mL)	A _V max _{24h} tumor (MBq/mL)	Follow-up tumor growth (days after ET start)
[Control]	1	A1	–	–	4
	2	A2	–	–	4
	3	A3	–	–	4
[ET]	1	B1	–	–	4
	2	B2	–	–	4
	3	B3	–	–	4
[PRRT]	1	–	3.10	7.13	10
	2	–	3.31	8.31	10
	3	C3	3.68	8.36	10
	4	C4	4.14	10.1	10
	5	C5	4.33	10.1	10
	6	–	5.56	13.2	10
	mean ± SEM	mean ± SEM	4.02 ± 0.36	9.53 ± 0.87	
		4.05 ± 0.19	9.52 ± 0.58		
[ET + PRRT]	1	–	3.32	8.11	10
	2	–	3.76	10.0	10
	3	D3	4.13	10.5	10
	4	D4	4.38	11.6	10
	5	D5	4.93	13.4	10
	6 ^R	–	7.22	18.0	11 ^E
	mean ± SEM	mean ± SEM	4.62 ± 0.57	11.9 ± 1.41	
		4.48 ± 0.24	11.8 ± 0.85		
[Control]	1	E2	–	–	4
	2	E2	–	–	4
	3	E3	–	–	4
[ET]	1	F1	–	–	4
	2	F2	–	–	4
	3	F3	–	–	4
[PRRT]	1	–	0.33	0.92	7 ^A
	2	G2	0.36	1.03	10
	3	G3	0.39	1.17	10
	4	G4	0.56	1.36	10
	5	–	0.59	1.53	10
	6	–	0.60	1.62	7 ^A
	7	–	0.70	1.66	10
	mean ± SEM	mean ± SEM	0.50 ± 0.05	1.33 ± 0.19	
		0.44 ± 0.06	1.19 ± 0.10		
[ET + PRRT]	1	–	0.39	1.04	10
	2	H2	0.47	1.32	10
	3	H3	0.56	1.45	10
	4 ^R	H4	0.88	2.22	10
	5 ^R	–	0.93	2.71	18 ^E
	6 ^R	–	1.04	3.17	18 ^E
	7 ^R	–	1.23	3.34	18 ^E
	mean ± SEM	mean ± SEM	0.79 ± 0.12 *	2.18 ± 0.35	
		0.64 ± 0.12	1.66 ± 0.28		

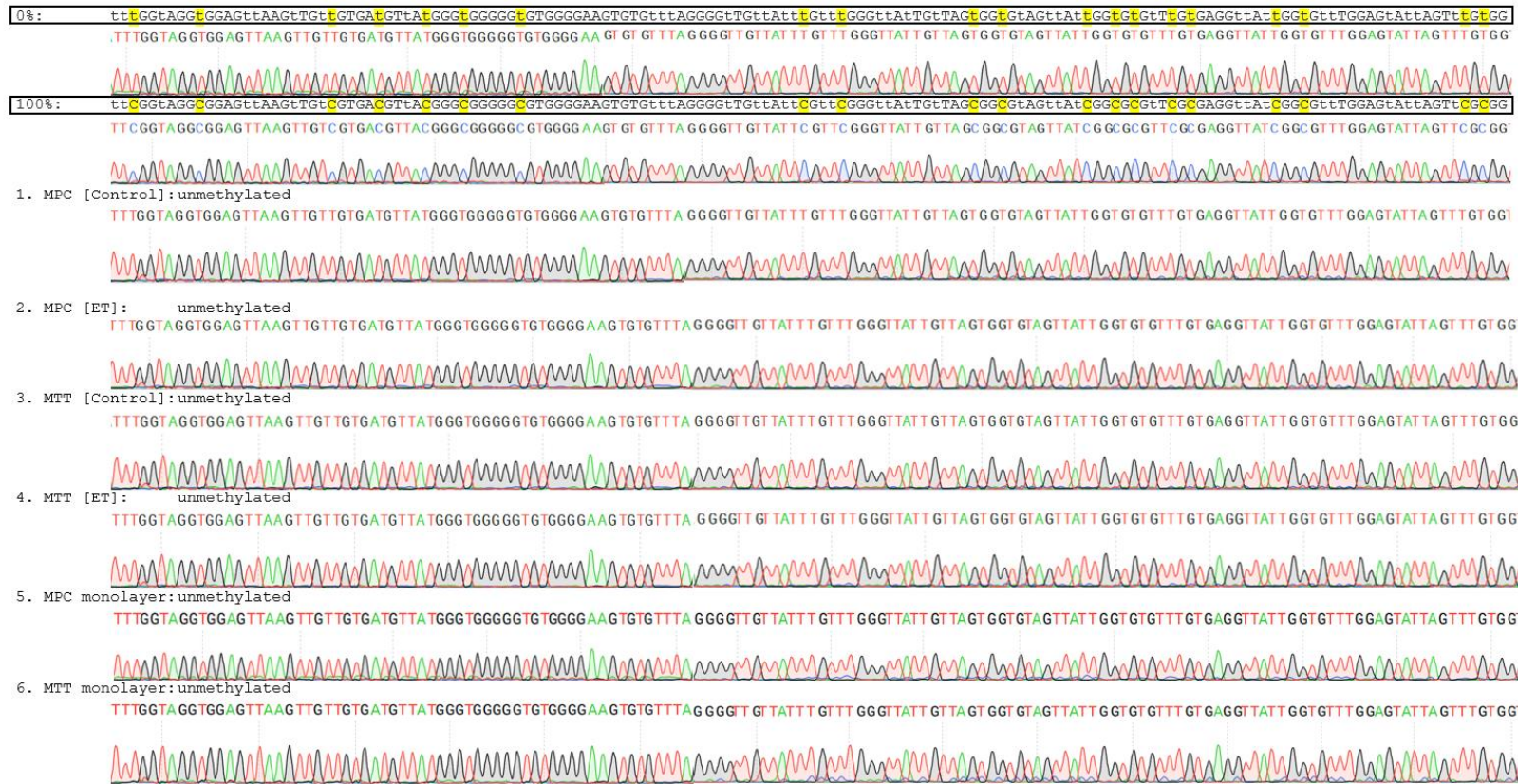
¹ Sample codes A–H can be found in the results section.

^R A_V responders to epigenetic treatment; responder thresholds were calculated from the mean A_V values of the [PRRT] cohorts + two times typical error (2×TE); significance of differences compared to [PRRT]: *P < 0.05

^A Aborted follow-up due to incidental death during imaging procedure

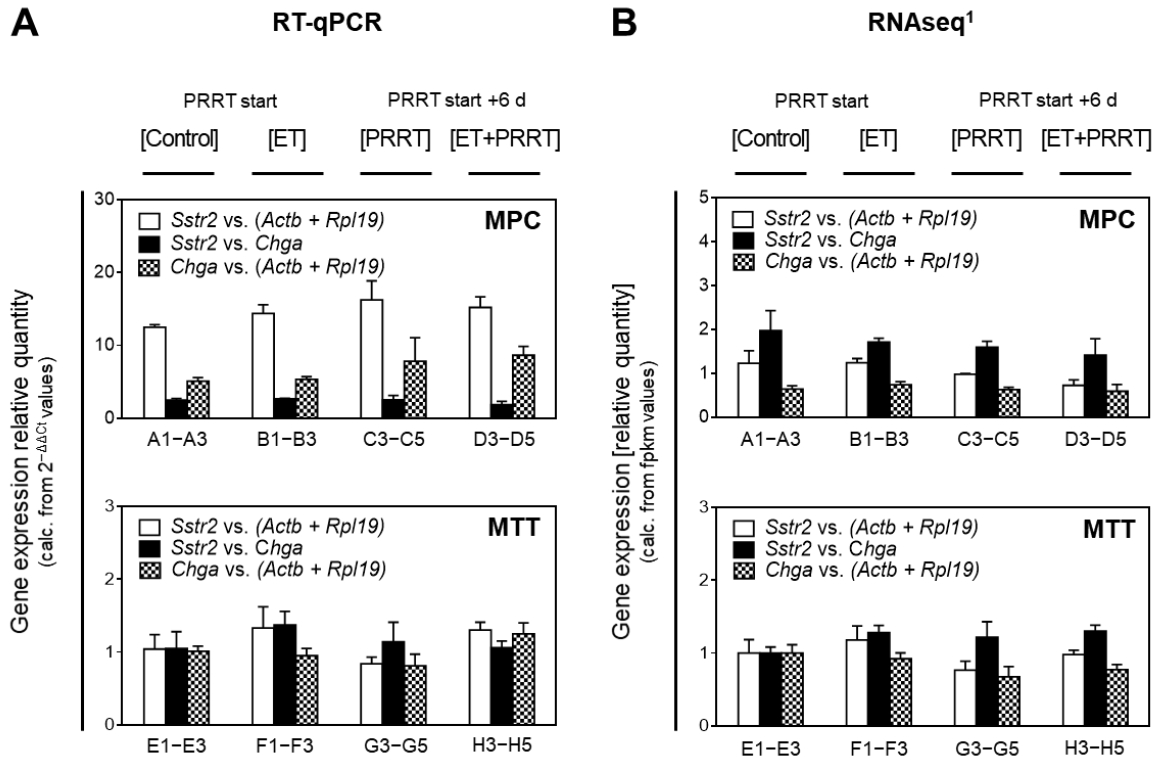
^E Extended follow-up in selected animals presenting with highest initial activity concentrations in tumor

261
262
263
264
265
266



268

269 **Figure S 7: *Sstr2* promoter methylation;** ET: treatment with VPA (250 mg/kg) and DAC (1 mg/kg) as combination doses on days 0 and 3; Genomic DNA from allograft tumors (1-4) or monolayer
 270 cultures (5-6) was extracted and treated with bisulfite. PCR products spanning 20 CpGs (highlighted in yellow) of the *Sstr2* promoter (amplified region 11:113510045-113510239,GRCm39) were
 271 generated and Sanger sequenced (forward and reverse) together with methylated (100%) and unmethylated (0%) control DNA. Representative examples of three different allografts per group are
 272 depicted.



273

274

275

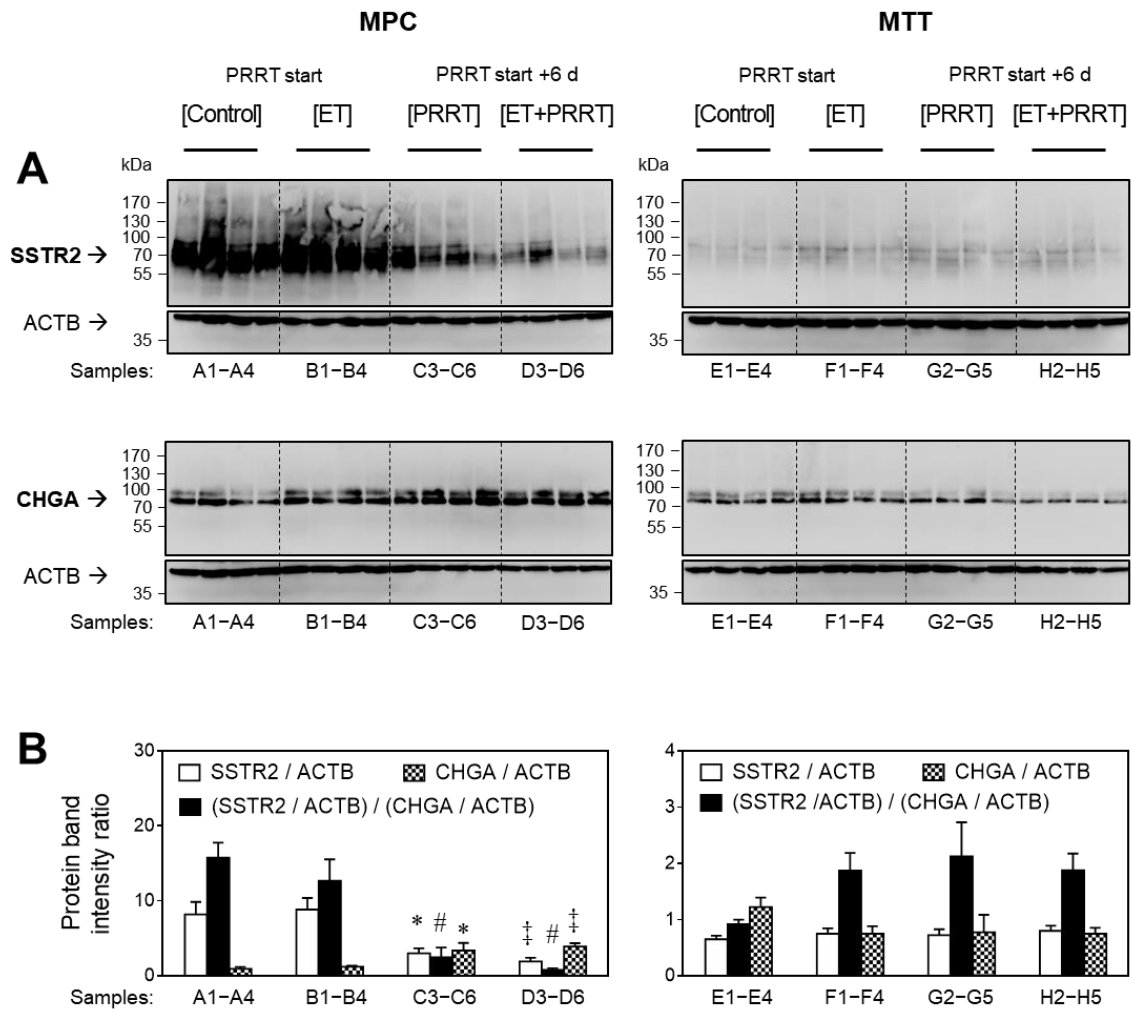
276

277

278

279

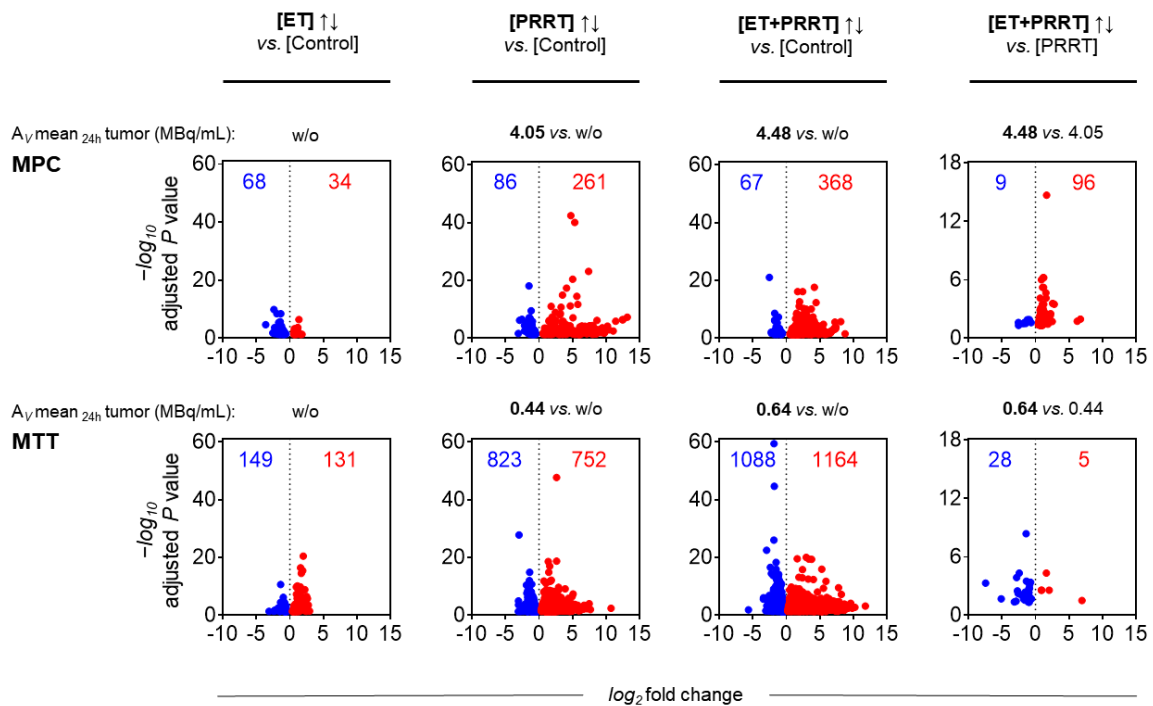
Figure S 8: Comparison of RT-PCR and RNAseq in gene expression analyses of selected genes in MPC and MTT tumors responding to treatments; ET: treatment with VPA (250 mg/kg) and DAC (1 mg/kg) as combination doses on days -4 and -1; PRRT: treatment with [¹⁷⁷Lu]Lu-DOTA-TATE (70 MBq/animal, equivalent to 1.2 nmol) as a single dose on day 0 (A) Relative gene expression ratios calculated from $2^{-\Delta\Delta C_t}$ values measured using RT-qPCR; (B) Relative gene expression ratios calculated from fpkm values (fragments per kilobase million) measured using RNAseq; all data were normalized to the average of MTT [Controls]; ¹ mRNA samples MPC and MTT tumors were analyzed in separate RNAseq runs



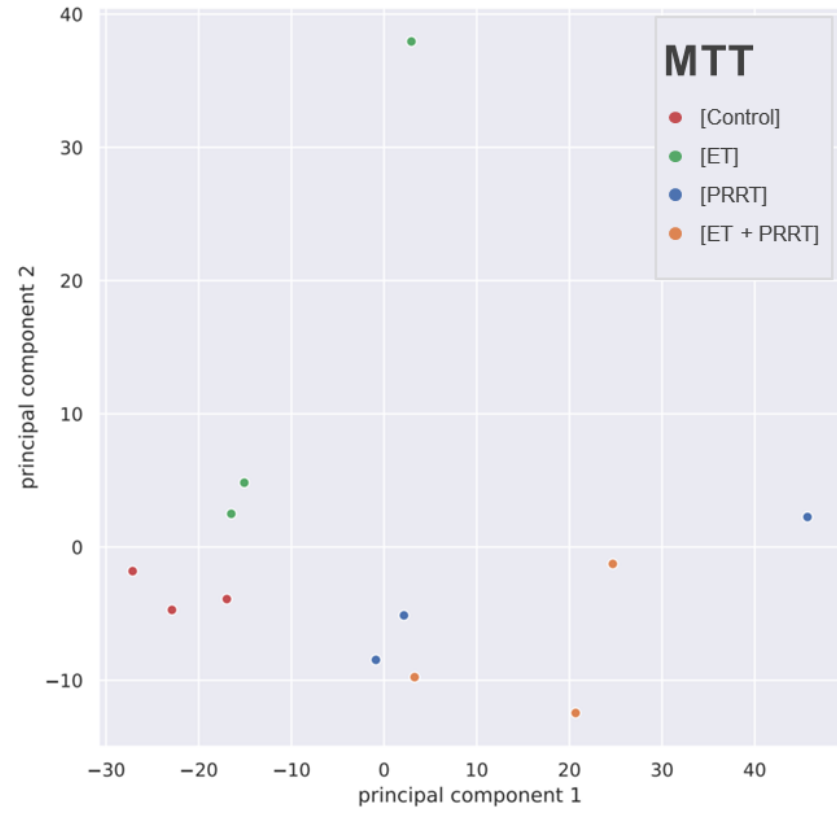
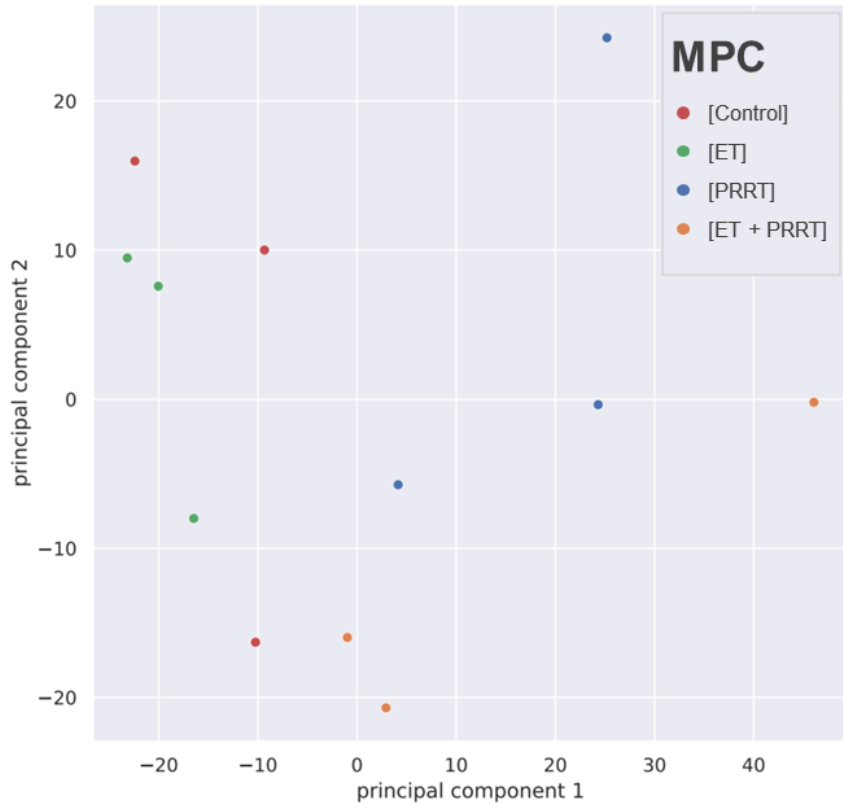
280
281
282
283
284
285
286
287
288

Figure S 9: Immunoblots analyzed for assessing SSTR2 and CHGA levels in tumors responding to treatments; ET: treatment with VPA (250 mg/kg) and DAC (1 mg/kg) as combination doses on days -4 and -1; PRRT: treatment with [¹⁷⁷Lu]Lu-DOTA-TATE (70 MBq/animal, equivalent to 1.2 nmol) as a single dose on day 0; (A) Total protein extracted from MPC tumors (14 µg/lane) and MTT tumors (24µg/lane) was separated using SDS polyacrylamide gel electrophoreses and blotted to PVDF membranes; immunodetection of SSTR2 and CHGA was done within the same experimental run on different membranes using identical concentrations of antibodies and developer substrate; (B) On each membrane, band intensities of the target proteins were normalized to ACTB as loading control; SSTR2/CHGA ratios were calculated from normalized target intensities; significance of differences: * $P < 0.05$; ‡ $P < 0.01$, # $P < 0.001$

289 2.5 Transcriptional responses of allograft tumors to epigenetic drugs and [¹⁷⁷Lu]Lu-DOTA-
 290 TATE – all genes and gene sets included



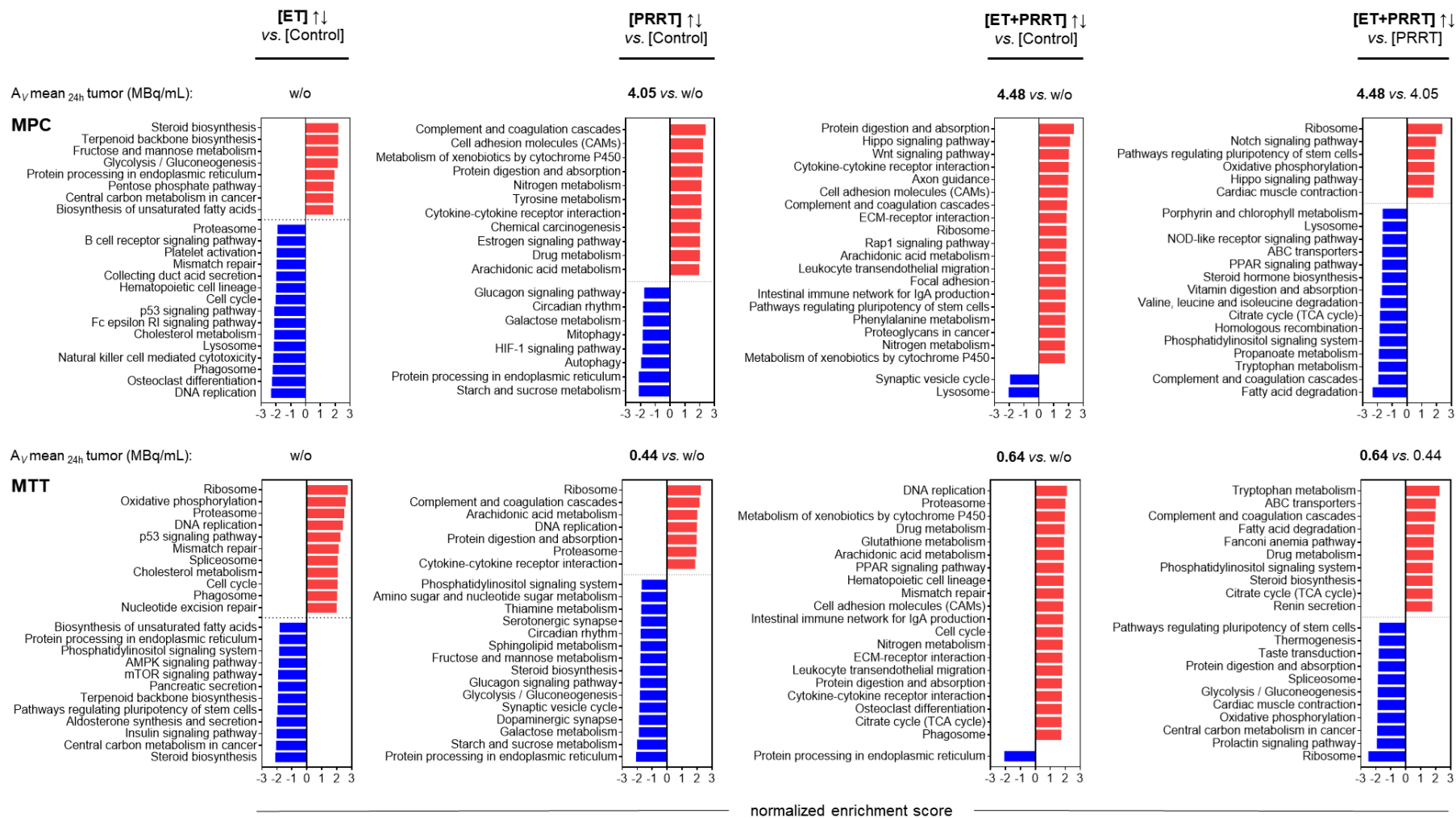
291
 292 **Figure S 10: Numbers of differentially expressed genes in MPC and MTT tumors in response to treatments; ET:**
 293 **treatment with VPA (250 mg/kg) and DAC (1 mg/kg) as combination doses on days -4 and -1; PRRT:**
 294 **treatment with [¹⁷⁷Lu]Lu-DOTA-TATE (70 MBq/animal, equivalent to 1.2 nmol) as a single dose on day 0; all protein-coding**
 295 **genes; $P_{adj} < 0.05$**
 296



297

298

Figure S 11: Principle component analysis of gene expression in MPC and MTT tumors responding to treatments; all genes included

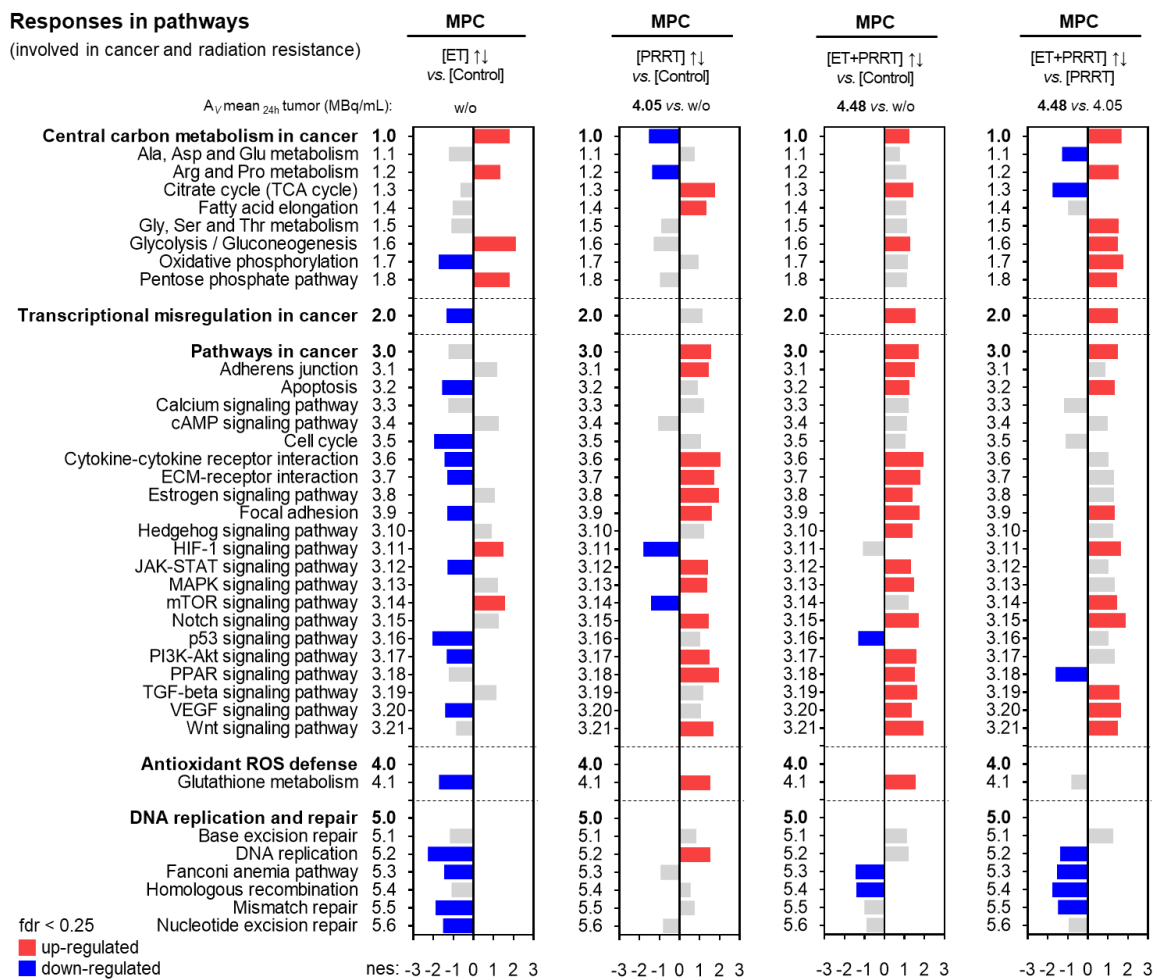


299
300
301

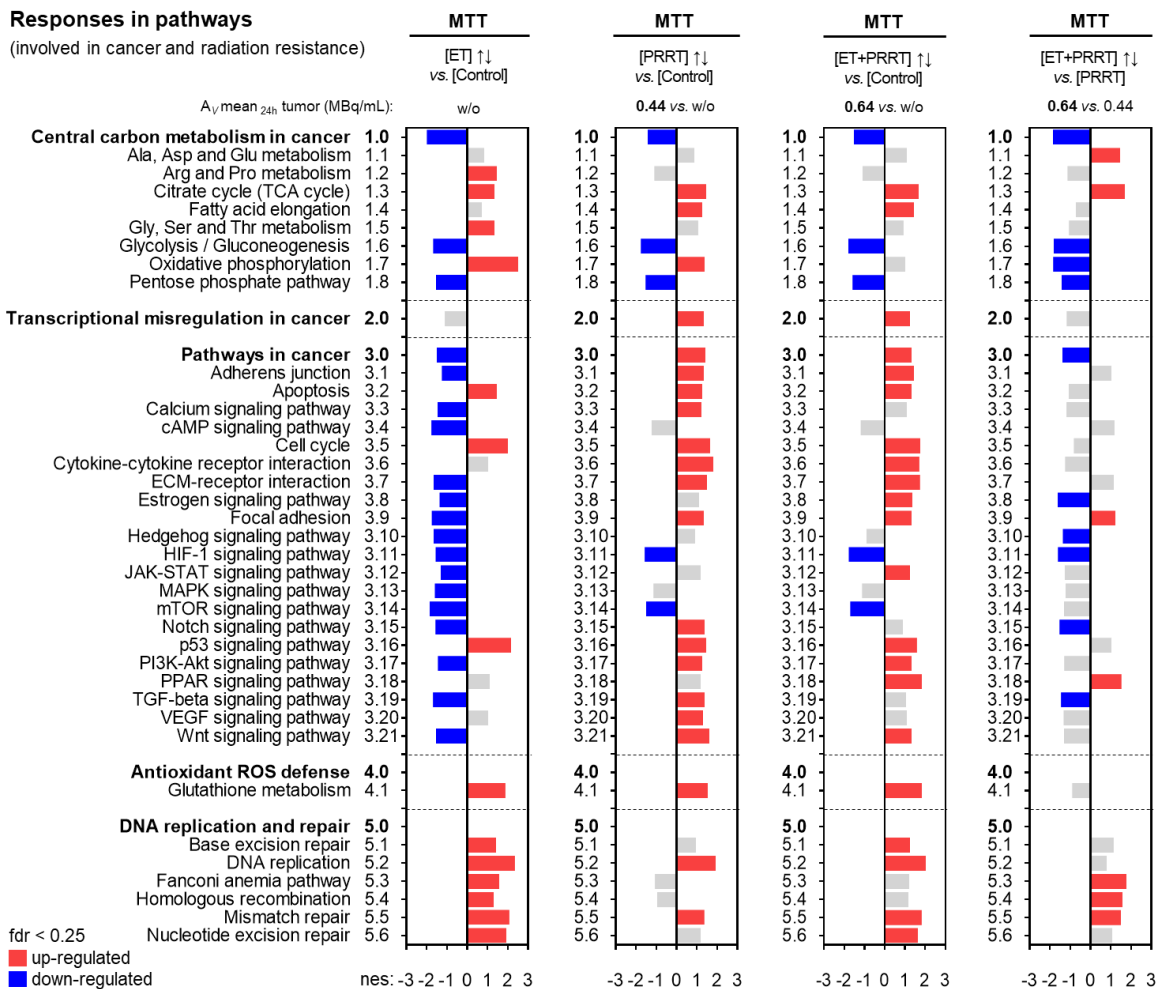
Figure S 12. Gene set enrichment analysis in MPC and MTT tumors – top-10 percent regulated gene sets in response to treatments; analysis based on KEGG pathway database; red bars: up-regulated pathways; blue bars: down-regulated pathways; pathways related to specific diseases have been excluded from the analysis; $\text{fdr} < 0.25$

302 2.6 Transcriptional responses of allograft tumors to epigenetic drugs and [¹⁷⁷Lu]Lu-DOTA-
 303 TATE – pre-selected gene sets involved in cancer and radiation resistance

304 Since the top-regulated gene sets in MPC and MTT tumors showed a number of pathways
 305 attributed to treatment-associated tissue damage and infiltration of leukocytes, a more specific
 306 pathway analysis was performed focusing on 39 pre-selected gene sets known to be involved
 307 in cancer and radiation resistance (see also Additional Methods 1.7).



308 **Figure S 13: Gen set enrichment in MPC tumors – treatment responses in pre-selected gene sets involved in cancer and**
 309 **radiation resistance; analysis based on KEGG pathway database; colored bars: fdr < 0.25; grey bars: fdr > 0.25**
 310

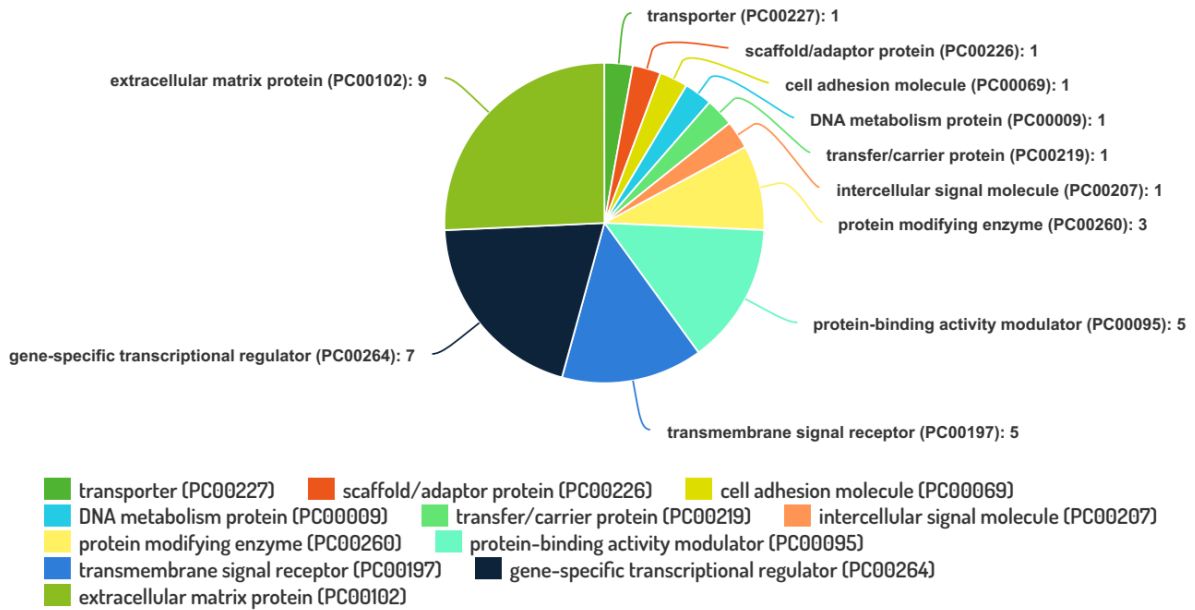


311

312

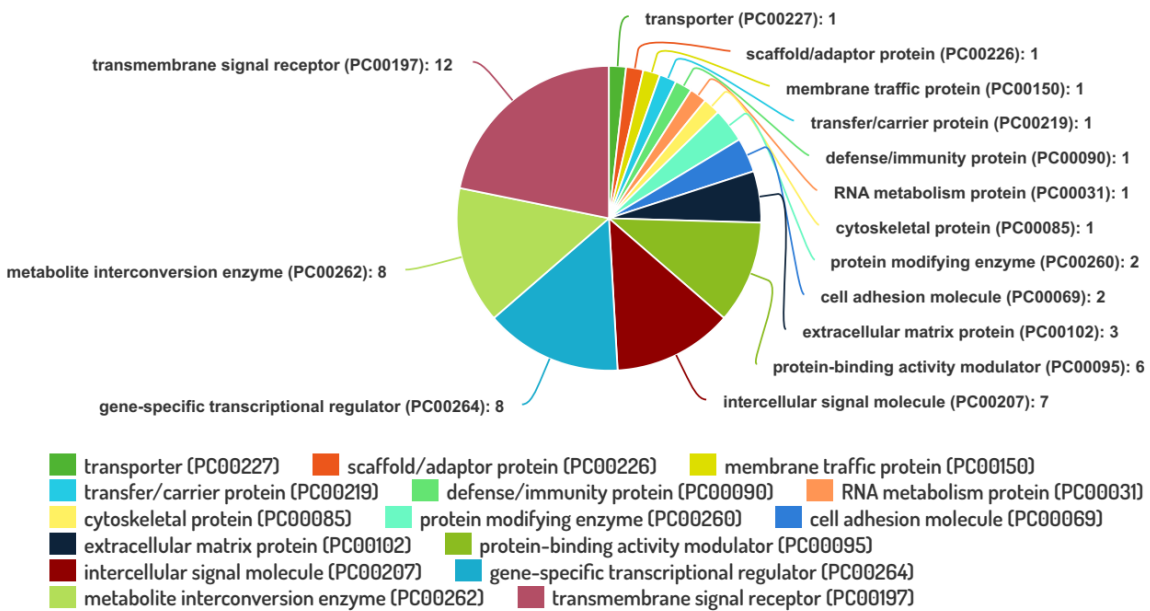
313

Figure S 14: Gen set enrichment in MTT tumors – treatment responses in pre-selected gene sets involved in cancer and radiation resistance; analysis based on KEGG pathway database; colored bars: fdr < 0.25; grey bars: fdr > 0.25



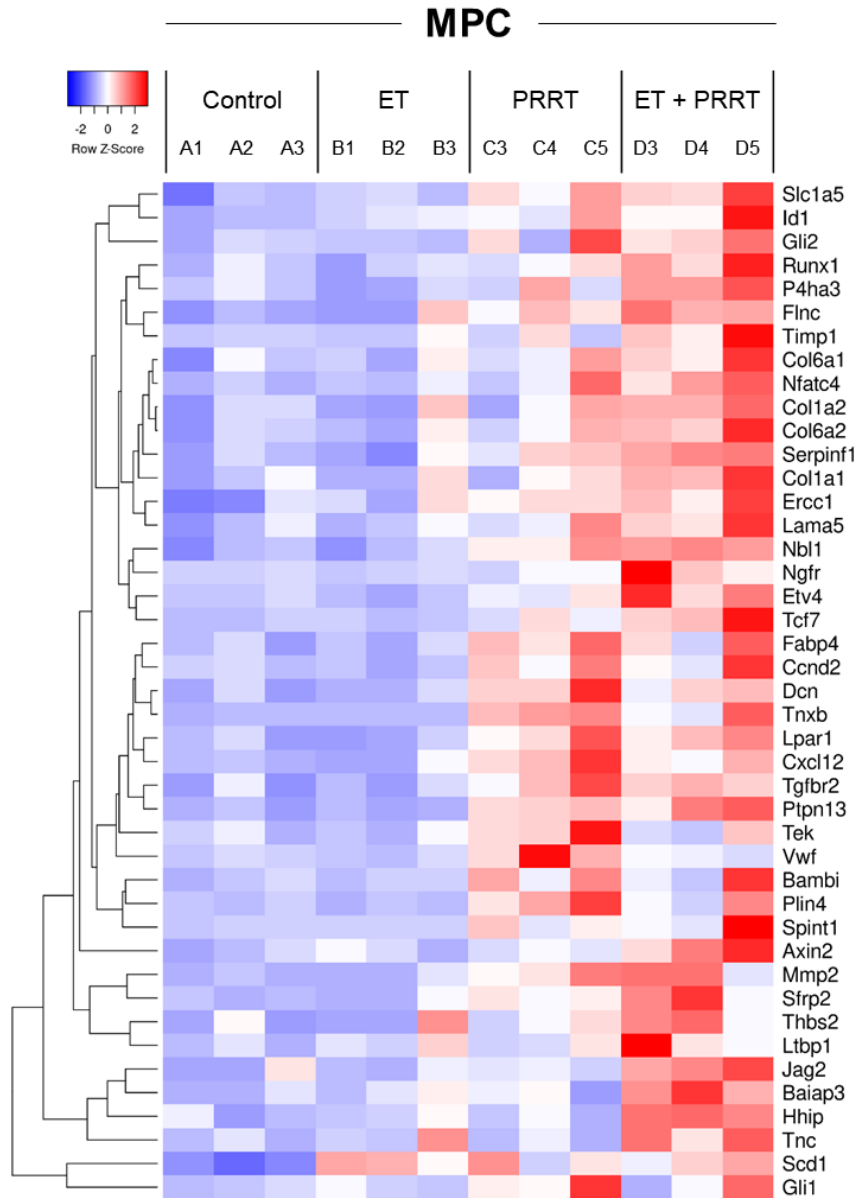
314

315 **Figure S 15: Protein classes encoded by leading-edge genes in MPC tumors responding specifically to $[^{177}\text{Lu}]\text{Lu-DOTA-}$**
 316 **TATE**; extracted from enrichment gene sets involved in cancer and radiation resistance; PANTHER gene list analyses based
 317 on gene ontology classification; $P_{\text{adj}} < 0.05$



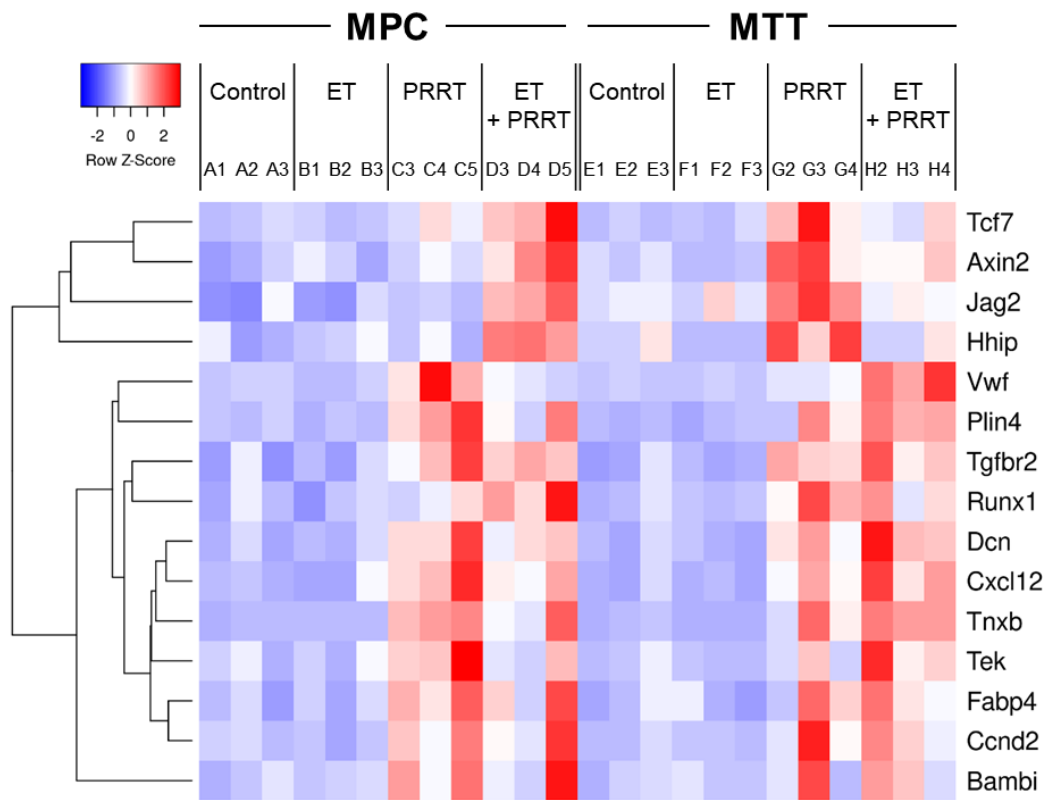
318

319 **Figure S 16: Protein classes encoded by leading-edge genes in MTT tumors responding specifically to $[^{177}\text{Lu}]\text{Lu-DOTA-}$**
 320 **TATE**; extracted from enrichment gene sets involved in cancer and radiation resistance; PANTHER gene list analyses based
 321 on gene ontology classification; $P_{\text{adj}} < 0.05$



322

323 **Figure S 17: Upregulated leading-edge genes in MPC tumors responding specifically to**
 324 **[¹⁷⁷Lu]Lu-DOTA-TATE; extracted from enrichment gene sets involved in cancer and**
 325 **radiation resistance; row clustering: average linkage of distances determined from Spearman**
 326 **rank correlation; $P_{adj} < 0.05$**



332

333 **Figure S 19: Upregulated leading-edge genes shared between MPC and MTT tumors responding**
 334 **specifically to [¹⁷⁷Lu]Lu-DOTA-TATE; extracted from enrichment gene sets involved in cancer and radiation**
 335 **resistance; row clustering: average linkage of distances determined from Spearman rank correlation; $P_{adj} < 0.05$**